J. Biochem. **143,** 685–693 (2008)
doi:10.1093/jb/mvn023

Interaction of Glutathione and Sodium Selenite *In vitro* Investigated by Electrospray Ionization Tandem Mass Spectrometry

Sheng-Yun Cui[1], Hua Jin[2], Seung-Jin Kim[2], Avvaru Praveen Kumar[2] and Yong-Ill Lee[2,*]

[1]Department of Chemistry of Yanbian University, Key Laboratory of Organism Functional Factor of the Changbai Mountain, Ministry of Education Yanji, 133002, China; and [2]Department of Chemistry, Changwon National University, Changwon 641-773, Korea

Received January 23, 2008; accepted February 8, 2008; published online February 22, 2008

Selenite has been found to be an active catalyst for the oxidation of sulphhydryl compounds, such as glutathione (GSH). Considering the biological importance of GSH oxidation and the implication of sulphhydryl compounds in selenium poisoning and other biological activities, more information on selenite oxidation of GSH in enzyme-free conditions is desirable. Herein, we describe glutathione and sodium selenite simply mixed in aqueous solutions. The interaction products and transient intermediate are identified and characterized using electrospray ionization (ESI) tandem mass spectrometry. In the first step, GSH directly reacts to form diglutathione (GSSG) and unstable selenodiglutathione (GS-Se-SG). Then selenodiglutathione further reacted with remaining GSH to form diglutathione and elemental selenium, Se^0. As the amount of GSSG significantly increased or acidity of the solution increased, the redox potential of glutathione [$E^{0'}$(GSSG/2GSH) ≈ -250 mV (NHE)] significantly shifted to the positive direction. This makes the GSSG react with elemental selenium formed in the solution, which can be demonstrated by another unstable intermediate ion identified at *m/z* 418 by mass spectrometry with the elemental composition of $[GSS\text{-}Se]^-$. The reaction mechanism between GSH and sodium selenite has been proposed according to the ESI-MS, NMR and UV-vis spectrometric measurements.

Key words: selenium, glutathione, sodium selenite; selenodiglutathione, electrospray ionization tandem mass spectrometry.

Abbreviations: GSH, Glutathione; GSSG, diglutathione; GS-Se-SG, selenodiglutathone; NHE, normal hydrogen electrode; RS-Se-SR, selenodisulfide; GS-Se-, selenopersulfide; DNA, deoxyribonucleic acid; ESI, electrospray ionization; MS, mass spectrometry; NMR, nuclear magnetic resonance; UV-Vis, ultraviolet-visible.

Sodium selenite is a common dietary form of selenium, which is recognized as essential in animal and human nutrition (*1*, *2*), but it can be highly toxic depending on its concentration and speciation (*3–5*). A number of selenium compounds have also been found to inhibit tumorigenesis in a variety of animal and cell models (*2*, *6–9*). Powerful cancer chemopreventive effects are seen for inorganic selenium salts, selenoamino acids and various synthetic organoselenium compounds. Selenite has been reported to be metabolized *in vivo* by glutathione (GSH) or glutathione reductase to hydrogen selenide (H_2Se) *via* selenodiglutathione and glutathionyl selenol intermediates (*10–13*). It has also been reported that the metabolism of selenium is dynamic and can be likened to *in vivo* combinatorial chemistry, in the sense that a wide array of products are formed with different intra-cellular environment (*10*).

GSH is a tripeptide of L-glutamate, L-cysteine and glycine and is a vital intra- and extra-cellular mammalian peptide with many biological functions (*14–19*), among them maintenance of the intra-cellular redox balance. GSH [$E^{0'}$(GSSG/2GSH) ≈ -250 mV (NHE)] is readily oxidized to glutathione disulphide (GSSG) and the GSH/GSSG ratio adjusts the global intra-cellular thiol redox potential. Most healthy cells have a GSH/GSSG ratio in the range of 100:1 (*16*, *17*). This ratio decreases during oxidative stress and disturbance of the GSH/GSSG ratio may affect proteins, DNA and membranes (*20–28*).

As GSH and selenite are highly redox active and this reaction is the main metabolic pathway of the selenite in mammals, the interaction between selenite and GSH is vital to biological activities and is related both with the beneficial and toxic effects on the organisms. So far, however, little information is available on the biological activity of selenium species, on their functions; most experiments on the topic have involved their activity while incorporated into selenoproteins. Therefore, to understand the detailed reaction mechanism,

*To whom correspondence should be addressed. Tel: +82-55-213-3436, Fax: +82-55-213-3439, E-mail: yilee.kr@gmail.com

$$4GSH + SeO_3^{2-} \longrightarrow GSSG + GS\text{-}Se\text{-}SG + 2OH^- + H_2O \quad (1)$$

$$GS\text{-}Se\text{-}SG + 2OH^- + O_2 \longrightarrow GSSG + SeO_3^{2-} + H_2O \quad (2)$$

Scheme 1. **Catalytic oxidation of GSH.**

$$4RSH + H_2SeO_3 \longrightarrow RS\text{-}Se\text{-}SR + RSSR + 3H_2O \quad (3)$$

Scheme 2. **Formation of selenodisulfide.**

identification of the interaction products and intermediates in a chemical approach are quite informative to get insight into the biological activities of the selenium.

Tsen and Tappel (*29*) reported that reduced glutathione is catalytically oxidized by selenite and proposed the sequence of reactions shown in Scheme 1 to explain the catalytic effect of Se^{4+}. However, whether the catalytic oxidation of thiol really proceeds as indicated in Scheme 1 with the regeneration of selenite in each cycle is open to question. Painter (*30*) observed the high reactivity of selenite with thiol groups. He is the first to demonstrate the formation of selenotrisulphide (RS-Se-SR), which is later renamed selenodisulphide, according to the reaction shown in Scheme 2.

Recently, Kessi and Hanselmann (*31*) investigated the reaction in the mixture solution with different ratios of GSH/selenite by dynamic UV-vis spectrometric measurements. In the samples with a starting GSH:selenite ratio >2, turbidity is visible in the absorption spectra within a few minutes after initiation of the reaction. The appearance of turbidity paralleled the formation of orange-red Se^0 particles. Higher turbidity correlated with higher initial selenite concentration and higher GSH:selenite ratio.

In recent years, the focus of research has been on peptides and their composition, with few investigators studying the fragmentation properties of single amino acids. Selenoamino acids have been examined by mass spectrometry (MS) (*32–34*), but characterization of selenium species in biological extracts by enhanced ion-pair liquid chromatography with inductively coupled plasma-MS and by referenced electrospray ionization (ESI) mass spectrometry (*35*), however, the use of the electrospray–ion trap combination for such studies is limited. The reaction between glutathione and selenite has been investigated by chemical approach and makes clear that the GSH directly oxidized to GSSG by selenite and various reduced selenium species, such as selenodiglutathione, elemental selenium and selenopersulphide of glutathione (GS-Se-), even though there is a lack of detailed information about the reaction mechanism. In this work, the mixture of sodium selenite and glutathione have been studied both in neutral and acidic solutions using ESI tandem MS to identify the interaction products and transient intermediates to interrogate the chemical interaction and detailed reaction mechanism in the solutions. The interaction products are characterized using MS^n tandem MS and dynamic UV-vis spectrometric measurements as well as NMR measurements. The regular changes of the relative abundances of interaction products in different acid media and incubation times of the mixture solutions are recorded by ESI mass spectrometer. The results indicate that the interaction between GSH and selenite is a dynamic redox reaction among the initial reactants and interaction products formed during the reaction. Dynamic UV-visible and NMR measurements suggested that a dynamic reaction takes place between GSH and sodium selenite, which depends on the acidity of the solution. The reaction mechanism has been proposed according to the experimental results.

EXPERIMENTAL PROCEDURES

Chemicals and Solutions—The glutathione, sodium selenite, other chemicals and solvents were purchased from Sigma–Aldrich (Milwaukee, WI, USA) and used as obtained, without further purifications. GSH and sodium selenite mixture solutions were prepared by mixing the stock solutions of sodium selenite and GSH solutions prepared in aqueous methanol (50/50%) as solvents just before measurements.

Instrumentation—ESI mass spectrometric experiments were performed using a LCQ-Advantage ion trap mass spectrometer (Thermo Finnigan) equipped with an electrospray interface. Operation conditions were as follows: spray voltage, 5 kV; capillary voltage, 46 V; heated capillary temperature, 200°C; and sheath gas (N_2), 15 arb. Helium gas admitted directly into the ion trap was used as the buffer gas to improve trapping efficiency and as the collision gas for CID experiments. Tube lens offset voltages were set by using a tune file created by auto tuning the LCQ on the interest ion signal, if not specified. Samples were infused using a syringe pump at a flow rate of 5 μl min^{-1}. UV-vis absorption spectra were taken on an UV 265 spectrometer (Shimadzu). NMR experiments were taken using Bruker AV-300 spectrometer in D_2O solvents.

RESULTS

ESI Mass Spectra Generated in the Mixture of GSH and Sodium Selenite—To identify the interaction products in the mixture solutions between GSH and sodium selenite, our initial work was to generate full mass spectra for GSH and GSSG in aqueous/methanol (50:50) solutions using negative mode (Fig. 1). GSH (Fig. 1a) produced deprotonated ion at *m/z* 306 $[GSH\text{-}H]^-$, deprotonated dimeric ion at *m/z* 613 $[2GSH\text{-}H]^-$, trimeric ion at *m/z* 920 $[3GSH\text{-}H]^-$ and tetrameric ion at *m/z* 1227 $[4GSH\text{-}H]^-$, respectively, while GSSG (Fig. 1b) produced deprotonated ion at *m/z* 611 $[GSSG\text{-}H]^-$ and deprotonated dimeric ion at *m/z* 1223 $[GSSG\text{-}H]^-$. No apparent fragment ions were observed for both GSH and GSSG in our experimental conditions in the ion source.

Figure 2a and b show ESI mass spectra initiated in the mixture of GSH and Na_2SeO_3 in aqueous methanol solutions with different incubation times before infusion of the mixture solutions into the ESI-MS spectrometer. As shown in Fig. 2a and b, several interaction product ions, such as deprotonated diglutathione (GSSG) and selinodiglutathione (GS-Se-SG) as well as their sodium adduct anions were observed. Deprotonated diglutathione anion and its sodium adduct anions were

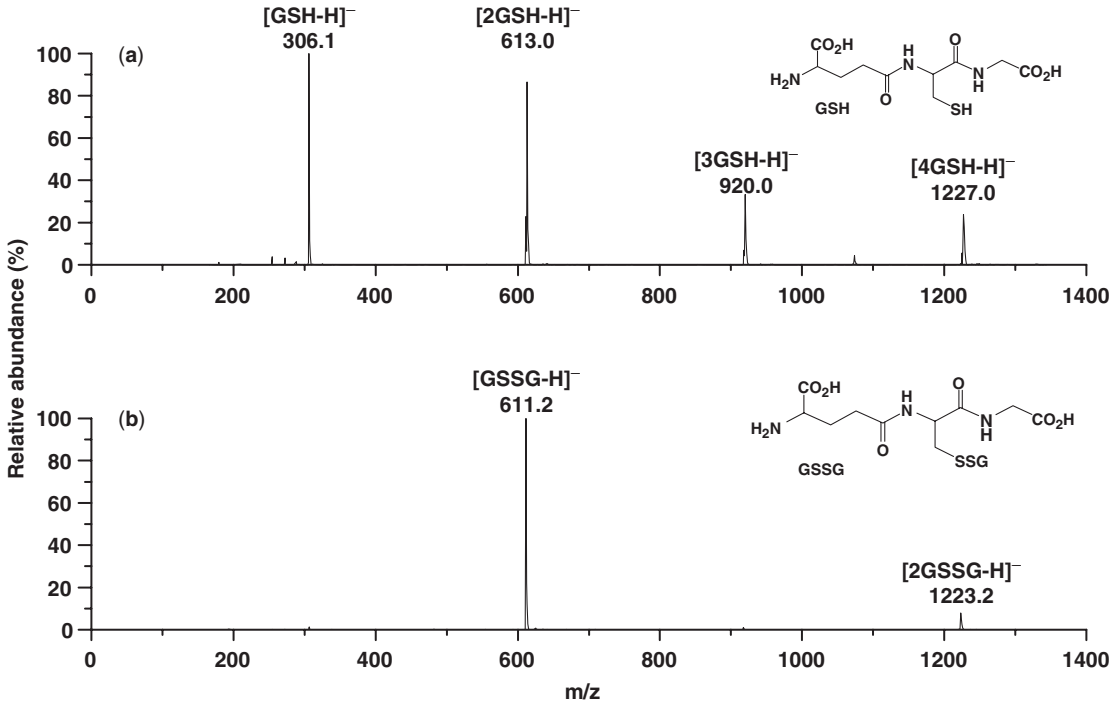

Fig. 1. **ESI mass spectra initiated in GSH (1 mM) (a) and GSSG (1 mM) (b) in aqueous/methanol (50:50) solutions in negative mode.**

observed at *m/z* 611.4 $[GSSG-H]^-$, at *m/z* 633.7 $[GSSG+Na-2H]^-$, at *m/z* 655.8 $[GSSG+2Na-3H]^-$ and at *m/z* 677.3 $[GSSG+3Na-4H]^-$, respectively with the tendency of increased total ion abundances as prolonged incubation time. Note also, the deprotonated selenodiglutathione $[GSSeSG-H]^-$ and its sodium adduct anions at *m/z* 691.4 $[GSSeSG-H]^-$, at *m/z* 713.2 $[GSSeSG+Na-2H]^-$ and at *m/z* 735.7 $[GSSeSG+2Na-3H]^-$, respectively. The abundances of deprotonated selenodiglutathione and its sodium adduct anions were decreased apparently with the prolonged incubation time. This implies that selenodiglutathione might decompose into the elemental selenium, Se^0 and diglutathione as was reported in the literature (*31*), which leads to fluctuation of the abundances of deprotonated diglutathione and selenodiglutathione as well as their sodium adduct anions. A minor anion peak in the initial reaction time with the element composition of $[GSSSe]^-$ was also recorded at *m/z* 418.4, which might be the unstable interaction intermediate between GSSG and elemental selenium, Se^0. The formation of elemental selenium can be confirmed also by the formation of minor turbidity of the solution in the initial reaction time and then the solution became apparent, which means that elemental selenium also takes part in the following reaction in the mixture solution.

To get insight into the reaction mechanism, the solution acidity of the interaction products, which greatly influences the redox potential of GSSG/GSH redox couple, has been investigated. Fig. 3a and b show the ESI mass spectra generated in 0.5% acetic acid (HAc) added in the same mixture solutions as in the same case shown in Fig. 2. The key ions generated from the mixture solutions shown in Figs 2 and 3 were summarized in Table 1. Several differences were observed in the different acidic solutions. Firstly, in the acidic solutions as shown in Fig. 3, the total abundances of the GSSG and its sodium adduct anions does not apparently increase with the prolonged incubation time as compared with aqueous methanol solutions shown in Fig. 2, while the abundances of the deprotonated selenodiglutathione and its sodium adduct anions in aqueous methanol solutions were apparently increased instead of decrease as in the case of relatively neutral solution shown in Fig. 2 (The relative abundance values were given in Table 1). Secondly, strong intermediate anion peak at *m/z* 418.4 with elemental composition of $[GSS-Se]^-$ was observed in the initial reaction time accompanied by a relatively higher abundance of deprotonated GSH anion at *m/z* 306.4. This anion peak at *m/z* 418.4 formed by the interaction between GSSG and element selenium might be an unstable intermediate anion because the abundance of the anion peak sharply decreased after incubation.

The results shown in Figs 2 and 3 imply that the reaction between GSH and sodium selenite was a dynamic redox reaction. The initial interaction products, such as GSSG and selenodiglutathone (GS-Se-SG) also take part in the following redox-reaction depending on the acidity of the solutions and relative amount of GSSG and GSH in the solution, which leads to the formation of selenium intermediate species, such as anion species at *m/z* 418 $[GSS-Se]^-$.

CID Mass Spectra for the Interaction Products—To characterize the structure of interaction products and intermediate formed, multiple stages CID mass spectra

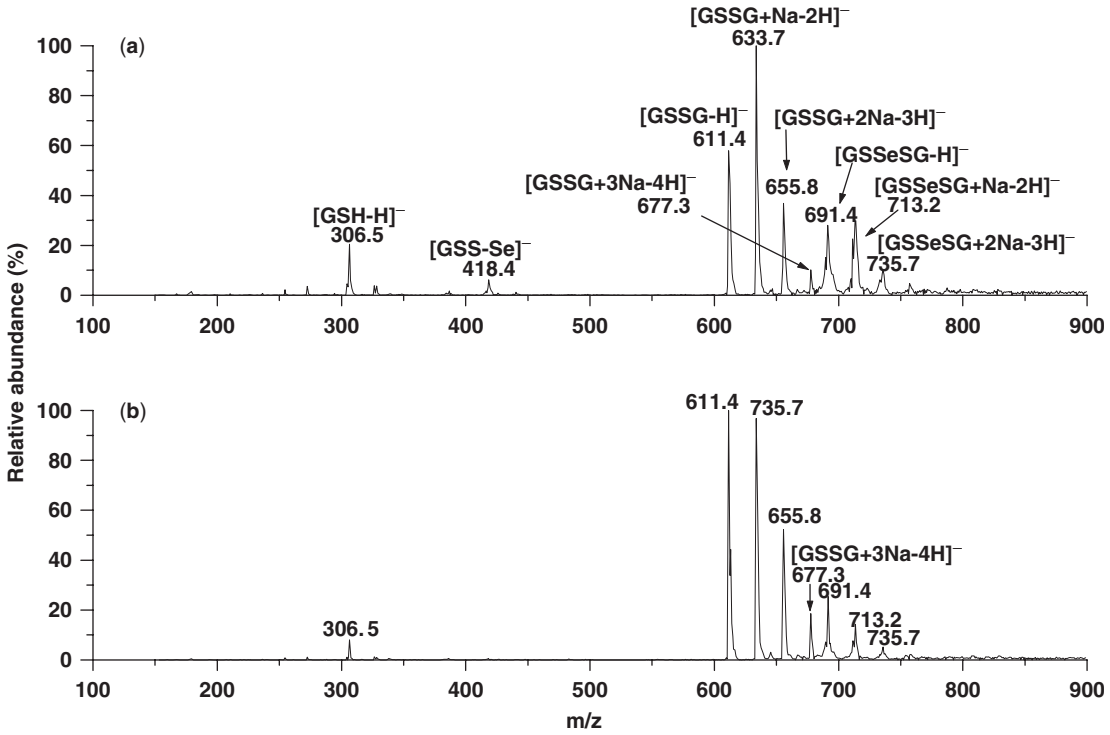

Fig. 2. **ESI mass spectra generated in the mixture solutions between GSH (5×10^{-4} M) and sodium selenite (5×10^{-4} M) in aqueous/methanol (50:50) solution using negative mode.** (a) Mass spectra obtained form the mixture solutions prepared just before the injection into spectrometer. (b) Mass spectra obtained after incubation of the mixture solution for 2 h at room temperature.

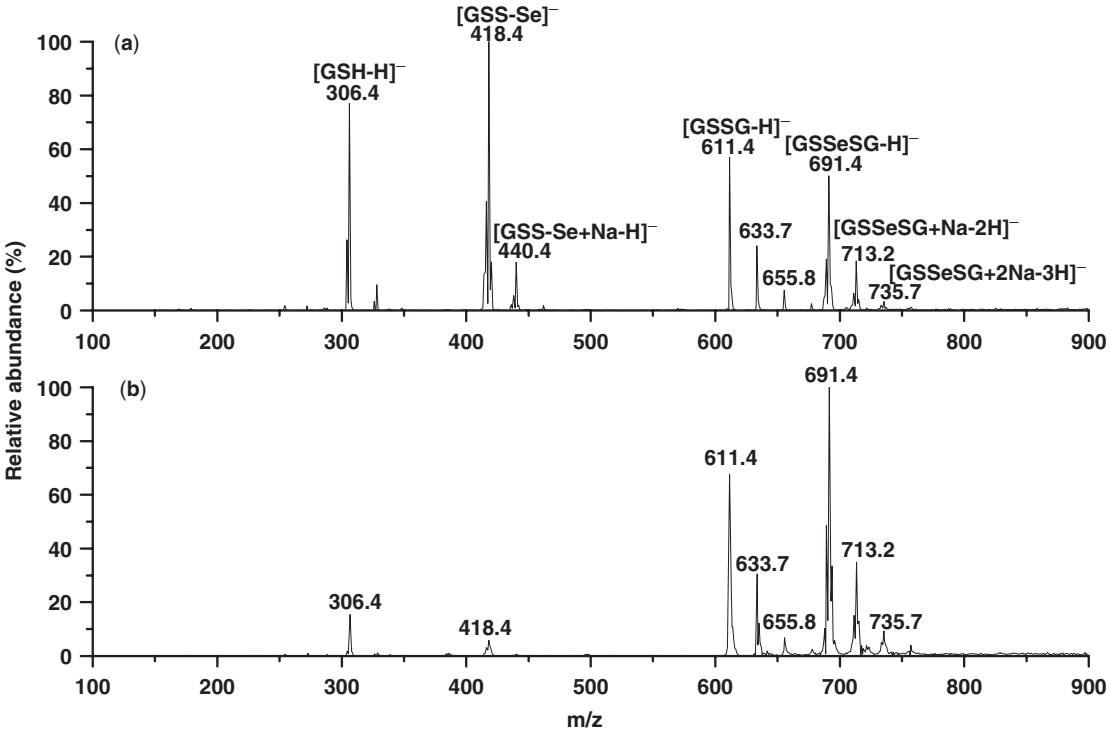

Fig. 3. **ESI mass spectra generated in the mixture solutions between GSH (5×10^{-4} M) and sodium selenite (5×10^{-4} M) with 0.5% acetic acid added in aqueous/methanol (50:50) solutions using negative mode.** (a) Mass spectrum obtained from the mixture solution prepared just before the injection into spectrometer. (b) Mass spectrum obtained after incubation of the mixture solution for 2 h at room temperature.

Table 1. **The abundances of key ions generated in the mixture solutions of GSH (5×10^{-4}M) and sodium selenite (5×10^{-4}M) with or without acetic acid added.**

	Ions (*m/z*)							
Time (h)	[GSH-H]$^-$ (306)	[GSSSeH-H]$^-$ (418)	[GSSG-H]$^-$ (611)	[GSSG+Na-2H] (634)	[GSSG+2Na-3H]$^-$ (656)	[GSSeSG-H]$^-$ (691)	[GSSeSG+Na-2H]$^-$ (713)	[GSSeSG+2Na-2H]$^-$ (736)
0	20.48	6.18	57.96	100	36.87	28.08	29.86	10.02
0[a]	77.10	100	57.02	24.08	7.48	50.10	18.38	3.36
2	8.0	0.57	100	95.88	51.99	25.33	14.23	5.13
2[a]	15.34	5.93	68.54	30.27	6.12	100	37.31	10.17

0 h represents the mixture solutions without incubation; 2 h represents the mixture solutions incubated 2 h before the sample infused into mass spectrometer.
[a]Represents the solutions with 0.5% acetic acid added.

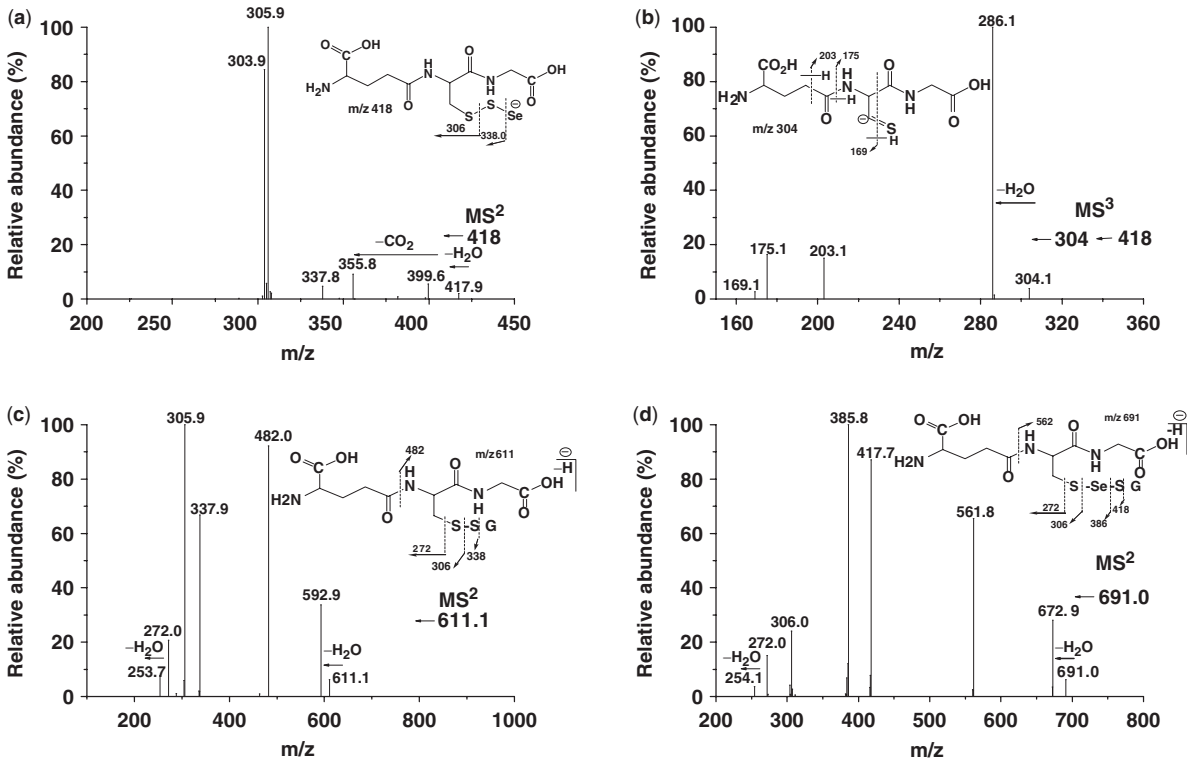

Fig. 4. **Multiple-stage CID mass spectra for the intermediate ion at *m/z* 418 [GSS-Se]$^-$, MS_2 CID mass spectra for the deprotonated diglutathione anion at *m/z* 611[GSSG-H]$^-$ and deprotonated selenodiglutathione anion at *m/z* 691 [GS-Se-SG-H]$^-$.**

for the product anions at *m/z* 418, *m/z* 611 and *m/z* 691 using activation conditions chosen to maximize fragment ion abundances were recorded as shown in Fig. 4. The structures of the interaction product ions and fragment patterns were also shown in the upper part of the Fig. 4. The anion at *m/z* 418 [GSS-Se]$^-$ (Fig. 4a), dissociated to the fragment ion at *m/z* 337.8 due to the loss of Se, indicating that selenium was not bound between two sulphur atoms. The relatively abundant fragment ion at *m/z* 304 was formed due to the loss of H_2SeS fragment from the precursor ion at *m/z* 418. This means the selenium attached to the sulphur easily withdraw hydrogen atom from GSH moiety during fragmentation. MS^3 CID mass spectra for the fragment ion at *m/z* 304 (Fig. 4b) further supported the fragment pattern shown in Fig. 4a. The fragment pattern for the deprotonated diglutathione at *m/z* 611 [GSSG]$^-$ and deprotonated selenodiglutathione at *m/z* 691 [GSSeSG-H]$^-$ coincide with the structures of diglutathione (GSSG) and selenodiglutathone (GSSeSG) suggested in the Fig. 4c and d.

Dynamic UV-vis and NMR Spectrometric Measurements—Similar results were observed from the dynamic UV-vis spectrometric measurements. Figure 5 shows dynamic UV-vis spectra and absorbance changes at 260 nm for selenodiglutathione initiated as the function of reaction time in different pH solutions. In the relatively neutral solution (Fig. 5a and c at pH = 6.63), the absorbance at 260 nm, which was typical absorbance band of selenodiglutathione (GS-Se-SG), decreased rapidly within the first minute of the reaction. It attained minimum within 10–25 min indicating that the selenodiglutathione formed in the initial reaction time apparently decomposed in the neutral solution. However, in the relatively acidic solution as shown in Fig. 5b and d

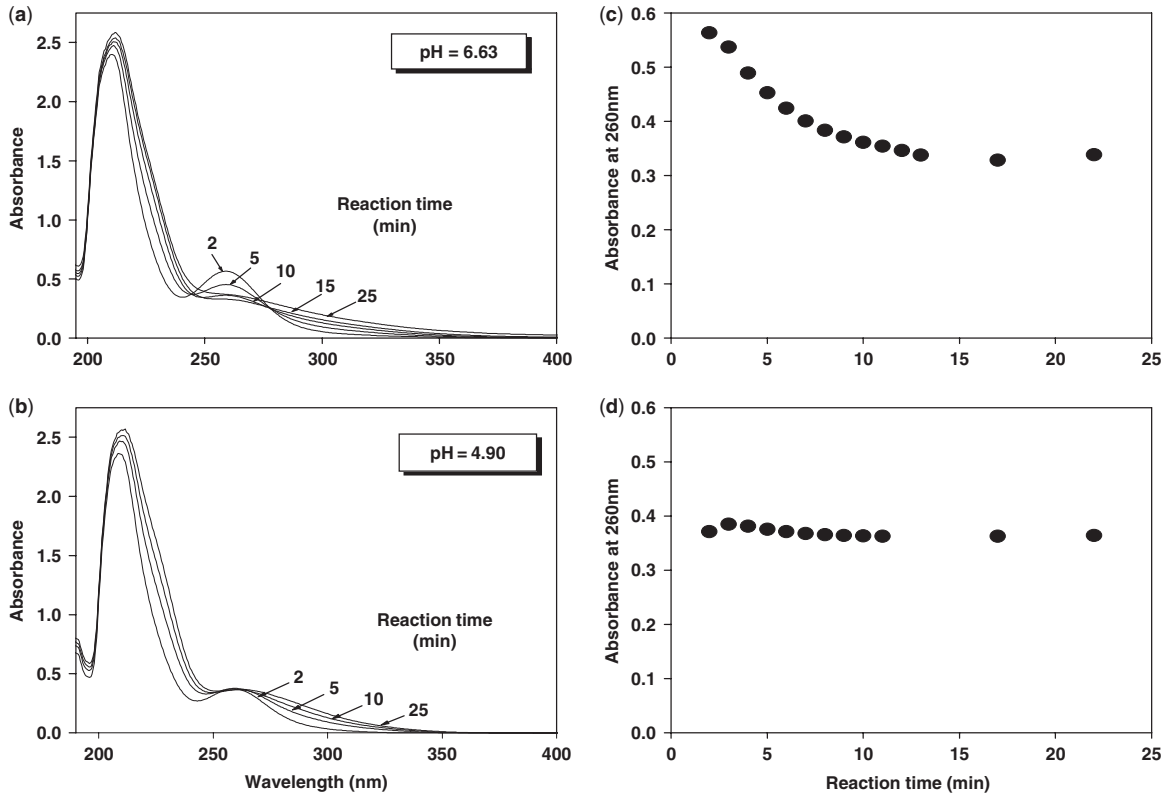

Fig. 5. **Representative absorption spectra of reaction mixtures illustrating the appearance and disappearance of selenodiglutathione in different pH solutions during the reactions.** The starting selenite concentration was 0.125 mM, GSH: selenite = 4:1. Formation of Se^0, which results in a visible increase in sample turbidity, can be seen at 400 nm after longer time of reaction where selenodiglutathione does not absorb.

the absorbance at 260 nm was not apparently decreased as the function of reaction time indicating that accumulation of selenodiglutathione takes place during the reaction. This means that the selenodiglutathione was more stable in the acidic solution.

In order to identify the final interaction products, ^{1}H NMR spectra were recorded for the GSH, GSSG and GSH+Na_2SeO_3 mixture in D_2O solutions with different acidic solutions. The relevant resonances were labelled in Fig. 6. The labelled hydrogen for GSH such as $CysH_\alpha$, $GlyH_\beta$, γ-$GluH_\alpha$, $CysH_\beta$, γ-$gluH_r$ and γ-$GluH_\beta$ have chemical shifts at $R = 4.43$, 3.85, 3.68, 2.82, 2.41 and 2.03, respectively (Fig. 6a) with the relative peak areas 1:2:1:2:2:2 which corresponds to the number of hydrogen atoms attached to the carbon atom. In the case of GSSG (Fig. 6b), apparent downfield shifts were observed for $CysH_\alpha$ and $GlyH_\beta$, and their spin coupling pattern changed significantly as compared to the results with GSH shown in Fig. 6a. The downfield shift and more complex spin coupling in GSSG were caused by the disulphide bond, hydrogen attached to chiral carbon $CysC_\alpha$ in different configuration within two GSH moieties because of the formation of hydrogen bonds. In the mixture solutions of GSH and Na_2SeO_3 with different acidity, different chemical shifts and coupling pattern were observed for $CysH_\beta$ (Fig. 6c and d). In the relatively neutral solution (Fig. 6d), ^{1}H-NMR spectrum was similar to the corresponding GSSG ^{1}H-NMR spectrum shown in Fig. 6b except upfield shift of $GlyH_\alpha$ and γ-$GluH_\alpha$ because of sodium adducted to adjacent protonated amino group, respectively. This means that the GSH final interaction product in the neutral mixture solution was dominantly GSSG. In the relatively acidic solution, $CysH_\beta$ was initiated another multiple peak around $\delta = 3.19$ indicating that ^{77}Se connected to sulphur atom in selenodiglutathione (GS-Se-SG) also takes part in the spin–spin coupling with $CysH_\beta$. This means that GSH final reaction products in the acidic mixture solution were dominantly GSSG and GS-Se-SG. These results were similar to the results measured by dynamic UV-vis spectrometry, where selenodiglutathione was easily decomposed in relatively neutral solution and stable in the acidic solution.

DISCUSSION

According to the Nernst equation shown in Scheme 3, the redox potential of glutathione was significantly influenced by the proton concentrations and the relative amounts of GSSG and GSH in the solution. In the relatively neutral solution, the redox potential was more negative than that of in the acidic solution indicating that GSH has more reductive properties and easily reacted with selenium species with higher oxidation number, such as selenite and selenodiglutathione with oxidation number of +4 and +2. In the acidic solution,

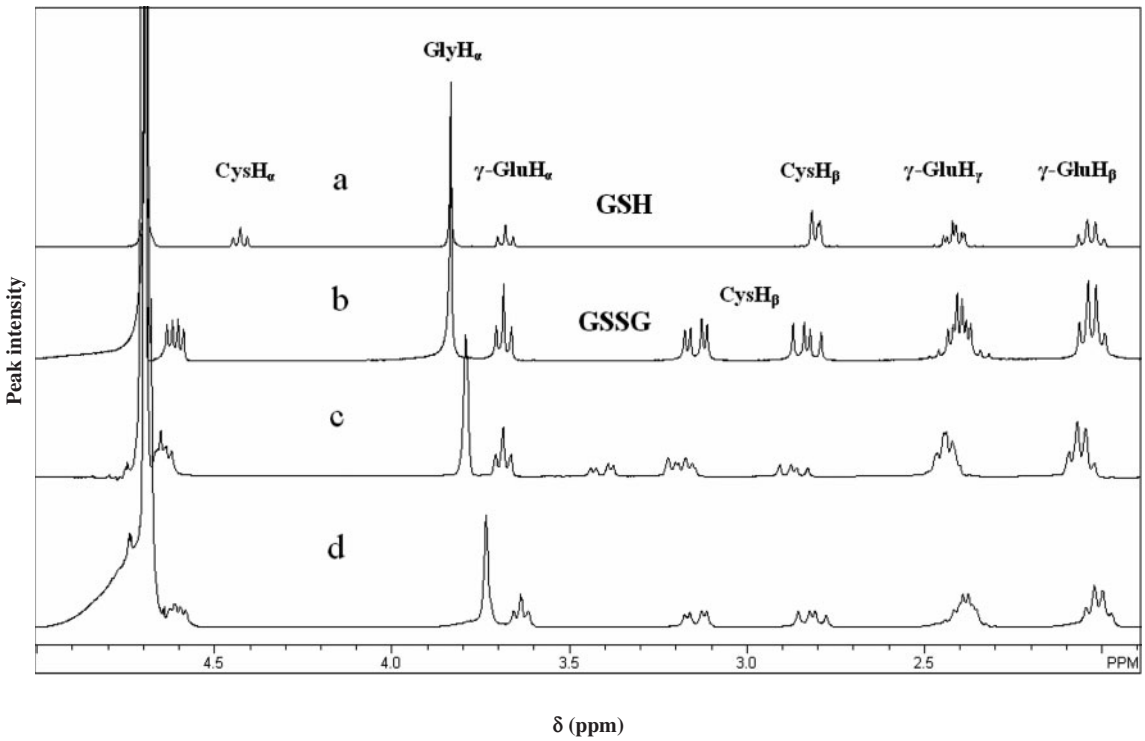

Fig. 6. **^{1}H-NMR spectra of solutions of GSH (a), GSSG (b), mixture solutions of GSH and Na_2SeO_3 in acidic (c) and neutral (d) heavy water (D_2O) solutions.**

$$GSSG + 2H^+ + 2e^- \rightleftharpoons 2GSH$$

$$E = E^0 + \frac{RT}{nF} Ln \frac{[GSSG][H^+]^2}{[GSH]^2}$$

$$(E^0\ (GSSG/2GSH) = -250mV(NHE))$$

Scheme 3. **Redox potential of glutathione from Nernst equation.**

however, the redox potential was shifted to positive direction because of higher proton concentration, which leads to the possibility of redox reaction between GSSG and selenium species with lower oxidation number such as elemental selenium (*31*, *36*), Se^0. The reaction between GSSG and elemental selenium was possible because nano-scale Se^0 was slightly soluble in the solution and also, according to the Pourbaix diagram (*37*), Se^0 has large thermodynamic stability in aqueous solution even in the relatively large negative potential. This means that the GSSG and the elemental selenium produced in the mixture solution were reacted with each other to form oxidized selenium species. In fact, transient intermediate selenium species was detected by ESI-MS spectrometer at *m/z* 418, $[GSS\text{-}Se]^-$ shown in Figs 2 and 3 might be the redox interaction product between GSSG and Se^0. From the results discussed above, the reaction mechanism was proposed as shown in Scheme 4.

As shown in Scheme 4, dynamic redox reactions with several steps take place in the mixture solutions of GSH and Na_2SeO_3, which depends both on the acidity of the solution and relative amount of GSSG/GSH. In the initial stage of the reaction, in the relative neutral solution, GSH reacted with sodium selenite to produce GSSG and selenodiglutathione (Step 1). Then unstable selenodiglutathione further reacted with remaining GSH to produce GSSG and Se^0. This explains why the abundances of deprotonated selenodiglutathione and its sodium adduct anion peak gradually decreased with the prolonged incubation time (Fig. 2), gradually decreased absorbance band at 260 nm (Fig. 5a) and only GSSG-related protons were detected in NMR measurements (Fig. 6). This means that the reactions of Steps 1 and 2 shown in Scheme 4 take dominant roles in the relatively neutral solution. In the acidic solution however, the redox reaction between GSSG and elemental selenium (Step 3) was profound because of oxidation properties of GSSG in acidic solution as discussed above and in fact, this reaction competes with decomposition reaction of selenodiglutathione (Step 2). As a result, very strong selenium intermediate anion peak at *m/z* 418 $[GSS\text{-}Se]^-$ was recorded in Fig. 3 with relative large abundances of deprotonated GSH ion peak at *m/z* 306. As the unstable selenium species formed in the Step 3 easily decomposed to GSH, which in turn reacted with remaining sodium selenite to produce GS-Se-SG and GSSG. Therefore, the final interaction products in acidic solution were GSSG and GS-Se-SG. This explains slightly decreased ion abundances for the deprotonated selenodiglutathione and its sodium adduct anions as the function of incubation time in the results shown in Fig. 3. Also, in

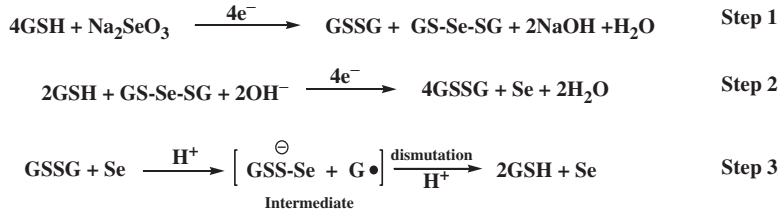

Scheme 4. **Reaction mechanism between GSH and Na_2SeO_3.**

the acidic solution, as Steps 1 and 3 reactions proceed dominantly, the accumulation of selenodiglutathione was possible. That explains why the relatively stable absorbance band at 260 nm (Fig. 5b), downfield shift and multiple coupling peaks for H_β (Fig. 6c) compared to H_β in GSSG.

CONCLUSIONS

Reduction of sodium selenite by GSH proceeds with two-step reduction reaction, which was greatly dependent on acidity of the solution. The acidity of the solution significantly influenced the relative redox potential between GSSG/GSH and redox couples of various selenium species. In the relatively neutral solution, sodium selenite was reduced to Se^{4+} species, selenodiglutathione and elemental selenium, Se^0 by the two-step reaction as shown in Scheme 4. In the acidic solution, GSSG has become more redox active with Se^0 and apparently produces unstable selenium intermediate species $[GSS\text{-}Se]^-$, followed by the dissociation into GSH and Se^0. In this case, Se^0 catalytically reduced GSSG to GSH *via* the transient intermediate $[GSS\text{-}Se]^-$. The interaction between GSH and sodium selenite was a dynamic reaction depending on the relative amount of GSSG/GSH and acidity of the solution, which leads to fluctuation of the GSSG/GSH ratio and the amount of selenium species, such as selenodiglutathione and elemental selenium in the solution. Therefore, it can be expected that the biological effects of sodium selenite including both beneficial and toxic effects to the mammalian depend on the biological environment, which leads to different selenium interaction species.

The authors gratefully acknowledge the support by the Korea Research Foundation (Grant No. KRF – 2004 – C00358).

REFERENCES

1. Combs, G.F. Jr. (1999) Chemopreventive mechanisms of selenium. *Med. Klin.* **94(Suppl. 3)**, 18–24
2. Combs, G.F. Jr. and Gray, W.P. (1998) Chemopreventive agents: selenium. *Pharmacol. Ther.* **79**, 179–192
3. Jacob, C., Giles, G.I., Giles, N.M., and Sies, H. (2003) Sulfur and selenium: the role of oxidation state in protein structure and function. *Angew. Chem. Int. Ed.* **42**, 4742–4758
4. Xu, J., Zhu, S.G., Yang, F.M, Cheng, L.C., Hu, Y., Pan, G.X., and Hu, Q.H. (2003) The influence of selenium on the antioxidant activity of green tea. *J. Sci. Food Agric.* **83**, 451–455
5. Wang, H.T., Yang, X.L., Zhang, Z.H., Lu, J.L., and Xu, H.B. (2002) Reactive oxygen species from mitochondria mediate SW480 cells apoptosis induced by Na2SeO3. *Biol. Trace Elem. Res.* **85**, 241–254
6. Gopalakrishna, R., Chen, Z.H., and Gundimeda, U. (1997) Selenocompounds induce a redox modulation of protein kinase C in the cell, compartmentally independent from cytosolic glutathione: its role in inhibition of tumor promotion. *Arch. Biochem. Biophys.* **348**, 37–48
7. Cristina, W.N., Gilson, Z., and Joao, B.T.R. (2004) Organoselenium and organotellurium compounds. *Toxicol. Pharmacol. Chem. Rev.* **104**, 6255–6285
8. Clark, L.C., Combs, G.F. Jr, and Turnbull, B.W. (1996) Effect of selenium supplementation for cancer prevention in patients with carcinoma of the skin: a randomized controlled trial. *J. Am. Med. Assoc.* **276**, 1957–1963
9. Thirunavukkarasu, C. and Sakthisekaran, D. (2003) Dietary micronutrient, prevents the lymphocyte DNA damage induced by *N*-Nitrosodiethylamine and phenobarbital promoted experimental hepatocarcinogenesis. *J. Cell. Biochem.* **88**, 578–588
10. Howard, E.G. (1999) Selenium metabolism, selenoprotein and mechanism of cancer prevention: complexities with thioredoxin reductase. *Carcinogenesis* **20**, 1657–1666
11. Gailer, J. (2002) Reactive selenium metabolites as targes of toxic metals/metalloids in mammals: a molecular toxicological perspective. *Appl. Organometal. Chem.* **16**, 701–707
12. Barbara, W., Halina, M.Z., and Pawel, N. (2001) Selenium compounds in the environment; their effect on human health. *Cell. Biol. Mol. Lett.* **6**, 375–381
13. Janine, K. and Kurt, W.H. (2004) Similarity between the Abiotic reduction of selenite with glutathione and the dissimilatory reaction mediated by Rhodospirillum rubrum and Escherichia coli. *J. Biol. Chem.* **279**, 50662–50669
14. Sies, H. and Ketterer, B. (1988) *Glutathione Conjugation: Mechanisms and Biological Significance,* Academic Press, London
15. Lees, W.J. and Whitesides, G.M. (1993) Equilibrium constants for thiol-disulfide interchange reactions: a coherent, corrected set. *J. Org. Chem.* **58**, 642–647
16. Akerboom, T.P., Bilzer, M., and Sies, H. (1982) The relationship of biliary glutathione disulfide efflux and intracellular glutathione disulfide content in perfused rat liver. *J. Biol. Chem.* **257**, 4248–4252
17. Fahey, R.C. (1977) Biologically important thiol-disulphide reactions and the role of cyst(e)ine in proteins: an evolutionary perspective. *Adv. Exp. Med. Biol.* **86A**, 1–30
18. Sies, H. (1999) Glutathione and its role in cellular functions – structural analysis of an engineered change in substrate specificity. *Free Radical Biol. Med.* **27**, 916–921
19. SchQfer, F.Q. and Buettner, G.R. (2001) Redox environment of the cell as viewed through the redox state of the glutathione disulfide/glutathione couple. *Free Radical Biol. Med.* **30**, 1191–1212
20. Christine, C.W. and Stephen, O.B. (1997) Characterization of the oxidation products of the reaction between reduced glutathione and hypochlorous acid. *Biochem. J.* **326**, 87–92
21. Sarita, C., Laxmayya, S., Vishal, S., Sandhya, P., Alka, S., and Digamber, I. (2005) Reduced glutathione: Importance

of specimen collection. *Indian J. Clinl. Biochem.* **20**, 150–152
22. Mine, E.I., Emine, S., and Gungo, K. (2002) Age-related changes in the glutathione redox system. *Cell Biochem. Funct.* **20**, 61–66
23. Pompella, A., Bahegyi, G., and Rousseau, M.W. (2002) *Thiol metabolism and redox regulation of cellular functions,* IOS Press, Amsterdam
24. Rajasekaran, N.S., Sathyanarayanan, S., Devaraj, N.S., and Devaraj, H. (2005) Chronic depletion of glutathione (GSH) and minimal modification of LDL in vivo: its prevention by glutathione mono ester (GME) therapy. *Biochim. Biophys. Acta* **1741**, 103–112
25. Mike, J.M., Teva, V., Chris, L., Marc, V.M., and Dirk, I. (1998) Glutathione homeostasis in plants: implications for environmental sensing and plant development. *J. Exp. Bot.* **49**, 649–667
26. Johanson, C., Lillig, C.H., and Arne, H. (2004) Human mitochondrial glutaredoxin reduces *S*-glutathionylated proteins with high affinity accepting electrons from either glutathione or thioredoxin reductase. *J. Biol. Chem.* **279**, 7537–7543
27. Sun, H.Z., Yan, S.C., and Cheng, W.S. (2000) Eur. interaction of antimony tartrate with the tripeptide glutathione. *J. Biochem.* **267**, 5450–5457
28. Ralf, D. (2000) Metabolism and functions of glutathione in brain. *Prog. Neurobiol.* **62**, 649–671
29. Tsen, C.C. and Tappel, A.L. (1958) Catalytic oxidation of glutathione and other sulfhydryl compounds by selenite. *J. Biol. Chem.* **223**, 1230–1234
30. Painter, E.P. (1941) The chemistry and toxicity of selenium compounds, with special reference to the selenium problem. *Chem. Rev.* **28**, 179–213
31. Kessi, J. and Hanselmann, K.W. (2004) Similarities between the abiotic reduction of selenite with glutathione and the dissimilatory reaction mediated by Rhodospirillum rubrum and Escherichia coli. *J. Biol. Chem.* **279**, 50662–50669
32. Kraus, R.J., Foster, S.J., and Ganther, H.E. (1983) Identification of selenocysteine in glutathione-peroxidase by mass-spectroscopy. *Biochemistry* **22**, 5853–5858
33. Ganther, H.E., Kraus, R.J., and Foster, S.J. (1984) Identification of selenocysteine by highperformance liquid chromatography and mass spectrometry. *Methods Enzymol.* **107**, 582–592
34. Block, E., Calvey, E.M., Gillies, C.W., Gillies, J.Z., and Uden, P.C. (1997) *Functionality of Food Phytochemicals,* Vol. 31, pp. 1–30, Plenum Press, New York and London
35. Mihaly, K., Susan, M.B., Julian, F., Eric, B., and Peter, C.U. (1999) Characterization of selenium species in biological extracts by enhanced ion-pair liquid chromatography with inductively coupled plasma-mass spectrometry and by referenced electrospray ionization-mass spectrometry. *Spectrochim. Acta B: At. Spectrosc.* **54**, 1573–1591
36. Ganther, H.E. (1971) Reduction of the selenotrisulfide derivative of glutathione to a persulfide analog by gluthathione reductase, *Biochemistry.* **10**, 4089–4098
37. Douglas, B.E., McDaniel, D.H., and Alexander, J.J. (1993) *Concepts and Models of Inorganic Chemistry*, QD475. D65, 2nd edn, pp. 580–581, John Wiley & Sons. Inc., New York